Ecological Indicators 107 (2019) 105545

Contents lists available at ScienceDirect

Ecological Indicators

journal homepage: www.elsevier.com/locate/ecolind

Trend-cycles of vegetation dynamics as a tool for land degradation assessment and monitoring

M.H. Easdale[a,*], C. Fariña[a], S. Hara[a], N. Pérez León[a], F. Umaña[b], P. Tittonell[a,c,d], O. Bruzzone[a]

[a] Instituto de Investigaciones Forestales y Agropecuarias Bariloche (IFAB), INTA-CONICET, Av. Modesta Victoria 4450 – CC 277 (8400), San Carlos de Bariloche, Río Negro, Argentina
[b] Instituto Nacional de Tecnología Agropecuaria (INTA), Bariloche. Argentina
[c] Groningen Institute of Evolutionary Life Sciences, Groningen University, PO Box 11103, 9700 CC Groningen, The Netherlands
[d] Agroécologie et Intensification Durable (AIDA), Centre de coopération Internationale en Recherche Agronomique pour le Développement (CIRAD), Université de Montpellier, 34000 Montpellier, France

ARTICLE INFO

Keywords:
NDVI trends
Desertification
Dryland
Monitoring systems
Wavelet

ABSTRACT

The use of time series of Normalized Difference Vegetation Index (NDVI), obtained from satellite sensors has become frequent in studies for land degradation assessment and monitoring. Linear trends of NDVI are usually considered as indicators of vegetation dynamics and widely used as proxies for land degradation. Yet, long-term trends of NDVI often exhibit unidirectional (monotonic) but also cyclic (non-monotonic) dynamics, including mid-term oscillations, both of which are poorly captured by linear trends. Trend-cycle is a time series analysis that represents a smoothed version of a seasonally adjusted time series, which provides information on long-term movements while including changes in direction underlying the series. We assessed NDVI trend-cycles in Patagonia (Argentina) as proxies for land dynamics, integrating trend and medium-term cycles (> 4 years). We used MODIS images between years 2000 and mid-2018; trend-cycles were analysed using the Basis Pursuit method. We observed that trend-cycles explained a significant portion of total temporal variability (reaching almost 20%), from which most patterns were explained by non-monotonic behaviour. We identified five major patterns in vegetation dynamics: decreasing (0.1% of area), increasing (0.6%), recovery (48.8%), relapsing (36.8%) and no trend-cycle (13.8%). Contrary to what is generally seen in the literature, monotonic patterns and particularly decreasing trend-cycles were marginally recorded in the last 18 years of NDVI records in Patagonia. Instead, the greater proportion of the area was classified as initial or advanced recovery and initial relapsing patterns, which refer to phases of a cyclic behaviour. We call for the need to revisit the conceptualization of land degradation assessment by means of remote sensing, and to critically review the ability of linear trends to reflect vegetation dynamics. Finally, we discuss the potential use of trend-cycle as a tool to monitor land dynamics and progress towards land degradation neutrality.

1. Introduction

Land degradation and desertification are among the most significant environmental problems in most arid and semi-arid regions worldwide (MEA, 2005). Monitoring systems are at the centre of demand to support decision-making and for impact assessment of intervention programs (Vogt et al., 2011), such as the Land Degradation Neutrality (LDN; Grainger, 2015). In particular, there is a need for relevant indicators for monitoring LDN as part of the Sustainable Development Goals (Hák et al., 2016). Current methodologies to monitor land degradation are under debate and efforts are increasingly oriented towards the development of accurate operative tools aimed at large areas in arid and semi-arid regions (Liu et al., 2015). Notwithstanding large and long-term regime shifts in ecosystem functioning, which are of high interest due to the relationship with degradation processes (Scheffer and Carpenter, 2003), arid rangeland dynamics exhibit also cyclic or periodic behaviour at different spatiotemporal scales, which are just too complex to be analysed with simple trend metrics (Peters et al., 2006). Rigorous and systematic approaches to addressing the complex, non-linear and large-scale dynamics of arid and semi-arid rangelands are still missing. In Patagonia, as in many other arid environments worldwide, there has not been any rigorous monitoring system of desertification processes during the last century. A recent proposal aimed at starting a regional field monitoring system named MARAS (Monitoreo

* Corresponding author.
E-mail address: easdale.marcos@inta.gob.ar (M.H. Easdale).

https://doi.org/10.1016/j.ecolind.2019.105545
Received 29 December 2018; Received in revised form 15 May 2019; Accepted 3 July 2019

Ambiental para Regiones Áridas y Semiáridas, in Spanish) provided a baseline with preliminary results (Oliva et al., 2019), which serves for future assessments of degradation and recovery processes at a landscape level. However, whereas these recent efforts are key to better tackling the problem in the future, there is a lack of regional information aimed at informing the magnitude, severity and rate of the process in the recent past.

Remote sensing provides opportunities to go back in the past to study ecological processes for which ground-based data were not recorded or were costly to obtain (Liu et al., 2015). The use of remote sensing data to monitor land degradation has several advantages such as a high resolution in space and time, spatiotemporal coverage, no extrapolation of data, low cost, permanent update and easy availability of data. Land degradation is usually defined as a long-term decline in ecosystem functioning and productivity loss caused by the interaction of human and environmental disturbances. Whereas it is a complex process, which should involve the assessment of different biophysical dimensions, productivity loss can be tackled by analysing trends of spectral indexes such as the Normalized Difference Vegetation Index (NDVI) estimated with satellite-sensed data series (Tucker, 1979). Most studies to date, however, use monotonic trends in NDVI as proxies for land degradation (Wessels et al., 2007; Bai et al., 2008; Metternicht et al., 2010). Indeed, several authors argued that land degradation trends can be adequately explained by monotonic functions such as linear trends (Eklundh and Olsson, 2003; Anyamba and Tucker, 2005; Vlek et al., 2008; de Jong et al., 2011; Beck et al., 2011; Omuto et al., 2014; Miao et al., 2012; Yin et al., 2012; Fensholt et al., 2012; Saha et al., 2015; Gaitán et al., 2015; Eckert et al., 2015; Luo et al., 2016; Zoungrana et al., 2018).

Recent research emphasizes some limitations of monotonic methods and trend analyses based on remotely sensed NDVI data for the detection of land degradation (de Jong et al., 2011; Wessels et al., 2012). Monotonic approaches do not consider neither states at dynamic equilibrium with a range of fluctuation nor hysteresis, two major limitations to assess long-term vegetation dynamics. A consequence of this methodological pitfall is the proliferation of alarmist conclusions associated with apparent regime shifts. Desertification as measured by significant negative linear NDVI slopes, or greening patterns by positive linear slopes, may be only apparent when contrasted against ground data or assessed through more complex trend analysis methods (cf. Easdale et al., 2018). There is a need to move forward in the analysis of non-linear vegetation change (Jamali et al., 2014). In particular, methods to assess land degradation through NDVI trends should be able to capture complex system dynamics by emphasizing the possibility of cyclic behaviours, and not only unidirectional processes.

The wavelet auto-regressive method (WARM) was recently proposed to classify NDVI trends (Easdale et al., 2018). This method was sensitive to capture both monotonic changes as potential references to regime shifts and non-monotonic changes depicted by cyclic dynamics, which can refer to different phases. Trend-Cycle Analysis (TCA) represents a smoothed version of a seasonally adjusted time series. Trend-cycles are frequently used by economists since they provide information on long-term movements, which includes changes in direction underlying the series. In macro-economic studies, one of the main aims is to distinguish between the forces that cause long-term growth and those that cause temporary fluctuations such as recessions (Nelson, 2010). In the field of land dynamics assessment, we propose trend-cycle as the combination of two distinct components: i) the trend, which accounts for long-term changes such as desertification, and ii) the cycle, which is a sequence of smoother fluctuations around the longer-term trend, in part characterized by alternating periods of expansion and contraction that refer to the phases of a cycle, such as wet and drought periods, respectively.

2. Desertification in Patagonia

The main process of land degradation that takes place in the arid and semiarid environments of Patagonia is termed desertification (MEA, 2005), which is a combination of soil erosion, loss of water bodies, vegetation, wildlife and human livelihoods. Notwithstanding the role of climatic factors in driving vegetation dynamics (Jobbágy and Sala, 2000), economic activities based on the exploitation of the natural resources such as hydrocarbons, mining and livestock production are at the core of the debates around land degradation in the region (Mazzoni and Vazquez, 2009). The regional severity of desertification in Patagonia was recorded in the past (del Valle et al., 1998). These authors estimated that 75.8% of Patagonia was affected by moderate to severe desertification. Other studies recorded degradation processes at plant community level (Aguiar et al. 1996; Oñatibia and Aguiar 2016), landscape (Verón and Paruelo, 2010) and regional scales (Gaitán et al 2013). During this period, a long-lasting drought affected most parts of the arid and semiarid region of Patagonia (varying spatially between 2008 and 2013; Villagra et al., 2008; Easdale et al., 2014), followed by above average annual rainfalls between 2014 and 2018. On the other hand, several volcanic eruptions generated ash fallout over different places and with varying magnitudes of ash deposits. The main events occurred in Northwest Patagonia: the Chaitén eruption in 2008 (Watt et al., 2009), Puyehue-Cordón Caulle Volcanic Complex eruption that generated the largest spatial ash deposits in 2011 (Collini et al., 2013), and the Calbuco eruption in 2015 (Van Eaton et al., 2016). These environmental circumstances and events were the main drivers of vegetation dynamics in Patagonia in the last two decades. We aimed at assessing NDVI trend-cycles in Patagonia (Argentina), as a method that integrates long-term trends and medium-term inter-annual cycles of vegetation dynamics. We apply the WARM model to NDVI time series for the period 2000 to mid-2018, obtained from MODIS images. Implications for large scale monitoring of land degradation processes are discussed.

3. Materials and methods

3.1. Study area

Patagonia is located between latitude 35° and 55° S. The extra-Andean Patagonia region is the largest arid and semiarid region of the southernmost portion of the American continent, which covers an area of approximately 550,000 km^2. There is a W-E biophysical gradient in terms of altitude (from 2000 to 400 m.a.s.l.) and rainfall (from 1000 to 200 mm yr^{-1}), which define 13 biozones (Paruelo et al., 1992; León et al., 1998). Whereas the Andean region is dominated by rainforest (*Nothofagus* spp.), the extra-Andean region is mostly dominated by grass-shrub and shrub steppes (Fig. 1; Bran et al., 2005). The largest biozones are the Central Plateau and Western Hills & Plateau steppes (51% of Patagonia) dominated by low shrubs and grasses, and the Monte shrublands (23%) (Fig. 1). Wetlands with very high productivity are frequent towards the Western sector, where they are used for livestock production, but they represent less than 3% of the total area (Bran et al., 2005). Smallholder pastoralism dominates in the North, with mixed herding of goat, sheep and cattle (Easdale et al. 2009), while larger ranches of sheep production dominate in the South.

3.2. Data source and processing

We used the 16–day composite MODIS images (MODIS13Q1 product) for the series February 2000–July 2018 obtained from the USGS Earth Resources Observation and Science (EROS) Data Centre. The sequences of clipped MODIS images (Hunter, 2007) were piled up into a space–time cube, from which the temporal sequence for each pixel along the last dimension of that matrix was obtained (i.e. time).

NDVI was derived from MODIS images, which was calculated with

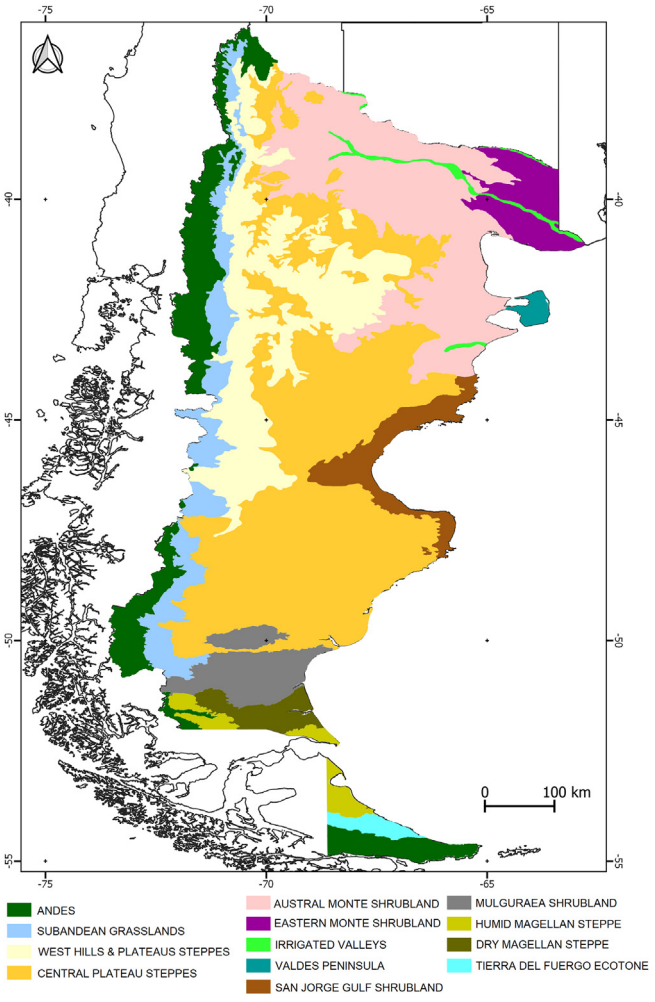

Fig. 1. Study area: Biozones of Patagonia, Argentina (Bran et al., 2005).

the following equation (Rouse et al., 1973):

$$NDVI = (\rho NIR - \rho R)/(\rho NIR + \rho R) \quad (1)$$

where ρNIR and ρR are the surface reflectances centered at 858 nm (near-infrared) and 648 nm (visible) portions of the electromagnetic spectrum, respectively.

We assumed that the NDVI error followed a logit-normal distribution (i.e. a statistical distribution whose logit transform follows a normal distribution; Ashton, 1972).

Before fitting the NDVI time series, data were logit-transformed in order to use a normal likelihood function. We treated NDVI values as a proportion between 0 and 1, using a normal function due to its simple interpretation and to avoid dealing with values larger than 1 or lower than zero. Then, we centred the series by removing the mean. Values lower than zero were treated as missing values because they are related to snow cover, clouds, water, rocks or non-vegetated ground. An additional criterion was that each pixel in the data stack consisting of *xy* NDVI layers that contained more than 20 negative values was discarded from the analysis. Most of the discarded pixels after performing this procedure corresponded to borders of water bodies and top of the mountains.

3.3. Trend-cycle estimations

We estimated NDVI-trend cycles at pixel level using an adaptive wavelet transform via the Matching Pursuit procedure. The Basis Pursuit algorithm decomposes a time series into an optimal weighted sum of time–frequency dictionaries based on the fewer coefficients norm (Chen et al., 2001), which most frequently are Gabor atoms (Demanet and Ying, 2007). A Gabor atom is a trigonometric function multiplied by a Gaussian window (Gabor, 1946):

$$g_{(t)} = a\cos(2\pi f(t-u))e^{\left(\frac{t-u}{\sigma}\right)^2} \quad (2)$$

where t is the time, a is the amplitude, f is the frequency of the trigonometric function, u is the centre of the atom, and σ is the standard deviation of the Gaussian window. By using a cosine, the periodic function was centred in the Gaussian window, so that the maximum of the window coincided with the maximum of the cosine (or minimum, depending on the amplitude sign). Then, any time series can be decomposed into a sum of these functions (Mallat, 1999). Information is compressed into optimal dictionary components, named Basis Pursuit. The main strength is that it combines the explanatory power of continuous wavelet transform (CWT) with a parsimonious representation, facilitating the interpretation and analysis of results.

The parameter u of the Gabor atoms was restricted to a range between 2000 (the beginning of NDVI time series) and 2019 (the end), whereas the frequency (f) was limited between positive and negative extremes by the nyquist frequency (23/2 year^{-1}) (Fig. 2).

At a pixel level and following the Basis Pursuit procedure, we used nonlinear regression via the Broyden-Fletcher-Goldfarb-Shanno (BFGS) algorithm (Fletcher, 1987) to calculate the parameters of the atoms. They were stepwise selected using the Corrected Akaike Information Criterion (AICc) (Hurvich and Tsai, 1989), as an acceptance versus rejection rule. The AICc was chosen because it corrects overfitting when the quotient between parameters (k) and number of data (n) is less than 40 ($n/k < 40$), and thus is an adequate decision rule for short time series. The atoms were progressively added until the AICc started increasing or 20 atoms was reached.

The sequence of atoms thus obtained was filtered, by means of the elimination of the atoms whose frequency was greater than 1/4 years. Then, the series were reconstructed with the remaining atoms, resulting in a low-pass filtering for which the high frequencies were eliminated, keeping only medium and long-term variability. The filtering and reconstruction of the series was done with the gpu_pursuit software version 0.02 (Bruzzone and Easdale, 2018), which implements the Basis Pursuit algorithm in a Graphical Processing Unit (GPU), by implementing the *in crowd* version of this algorithm (Gill et al., 2011) and allows fast calculations for large areas.

Trend-cycle atoms contained a periodic function, because we restricted the centre to be located within the span of the time series. Then, each function had at least one minimum and one maximum value within the span of the time series. Hence, the trend-cycle can represent both monotonic and non-monotonic functions, since its minimums and/

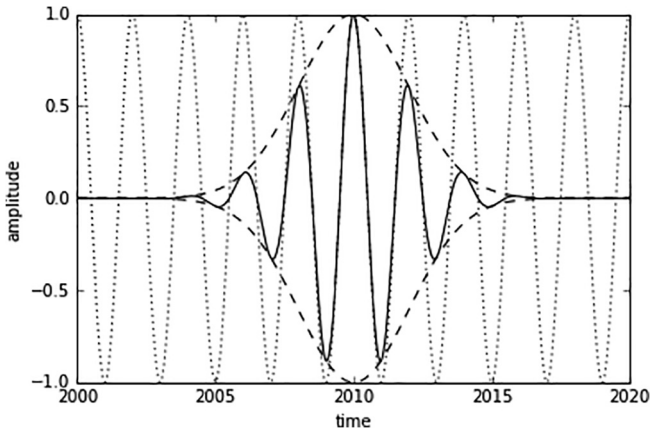

Fig. 2. Example of a Gabor atom centred in year 2010, with parameters f = 0.5 (two years wavelength) and σ = 2 years (see Eq. (2)).

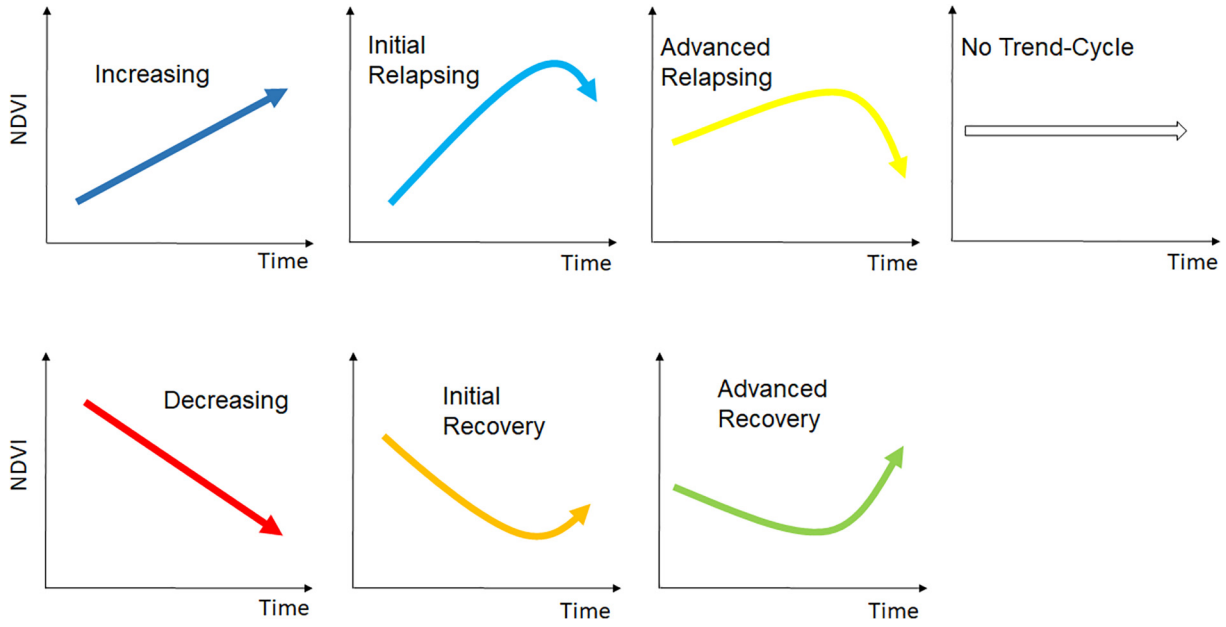

Fig. 3. Schematic representation of the classes of NDVI Trend-Cycles. Colour of the arrows represent the colours used in the map to identify pixels with different trend-cycles.

or maximums can be found anywhere in the time series. In order to classify different kinds of trend-cycles, we used as a rule the location of the maximum value with respect to the location of the minimum value in the time series (Fig. 3).

We defined seven classes of NDVI trend-cycles based on the position of minimum and maximum values in the series, as follows (Table 1): Increasing, Initial Relapsing, Advanced Relapsing, Decreasing, Initial Recovery and Advanced Recovery, No Trend-Cycle. A schematic representation of NDVI trend-cycles is shown in Fig. 3.

For the purpose of this paper, Increasing and Decreasing patterns were treated as monotonic trend-cycles, whereas the different types of recovering and relapsing trend-cycles were considered as non-monotonic functions, which described different positions of cyclic phases. We defined a framework of cyclic phases and transitions based on these non-monotonic functions, following the logic of sequencing among different trend-cycles (Fig. 4). Cyclic phases are represented, on the one hand, by the Positive phase, comprised by Advanced Recovery and Initial Relapsing trend-cycles, which refer to positive entry and departure stages, respectively. On the other hand, the Negative phase is comprised by Advanced Relapsing and Initial Recovery trend-cycles, which refer to negative entry and departure stages, respectively. Transition phases are represented by the Positive transition, comprised by Initial and Advanced Recovery trend-cycles, which refer to a positive early stage and a positive consolidated stage, respectively. The Negative transition is comprised by Initial and Advanced Relapsing trend-cycles, which refer to a negative early stage and a negative consolidated stage, respectively. The proportion of pixels (and area) classified by these different phases described the trend-cycles for Patagonia and its different biozones.

4. Results

Trend-cycle explained a significant portion of NDVI temporal variability, reaching almost 20% for Patagonia. Monotonic patterns were marginally recorded (< 1% of Patagonian area), highlighting that linear shifts were not dominant in the last 18 years of NDVI records. On the other hand, non-monotonic patterns or cyclic movements dominated vegetation dynamics (86% of total area), whereas areas with No Trend-Cycles accounted for almost 14% (Table 2).

Most frequent NDVI trend-cycles in Patagonia were Initial Relapsing (36%) Initial Recovery (30%), and Advanced Recovery (19%) (Table 2, Fig. 5). This means that Patagonian vegetation dynamics were mostly dominated by a changing phase that accounted for minimum NDVI values in the midsection of the time series, followed by increasing

Table 1
Classes of NDVI trend-cycles, colour in the map (Fig. 4) and description of main features.

Class	Colour	Description
Increasing	Blue	The maximum value occurred after the minimum value, and maximum was located at the end of the time series
Initial Relapsing	Light blue	Increasing time series whose maximum occurred at least one year before the end of the time series, and after the maximum a change in the trend direction occurred. This class represent initial stages of change in the direction from expansion towards retraction, suggesting a potential forwarding change to another phase
Advanced Relapsing	Yellow	Increasing time series whose maximum occurred at least one year before the end of the time series, and after the maximum a change in the trend direction occurred, followed by minimum values at the end of the time series. This class represent a consolidated change from a phase of expansion or growth that occurred in the middle of the series, towards a phase of retraction or contraction
Decreasing	Red	Decreasing time series, where the minimum value occurred after the maximum value, and minimum was located at the end of the time series
Initial Recovery	Orange	Decreasing time series whose minimum occurred at least one year before the end of the time series, and after that minimum, a change in the trend direction occurred. This class represent initial stages of change in the direction from retraction to expansion, suggesting a potential forwarding change to another phase
Advanced Recovery	Green	Increasing time series whose minimum values occurred at least one year before the end of the time series, and after the minimum a change in the trend direction occurred, followed by maximum values at the end of the time series. This class represent a consolidated change from a phase of retraction or contraction that occurred in the middle of the series, towards a phase of expansion or growth
No Trend-Cycle	White	Time series with not significant trend-cycle

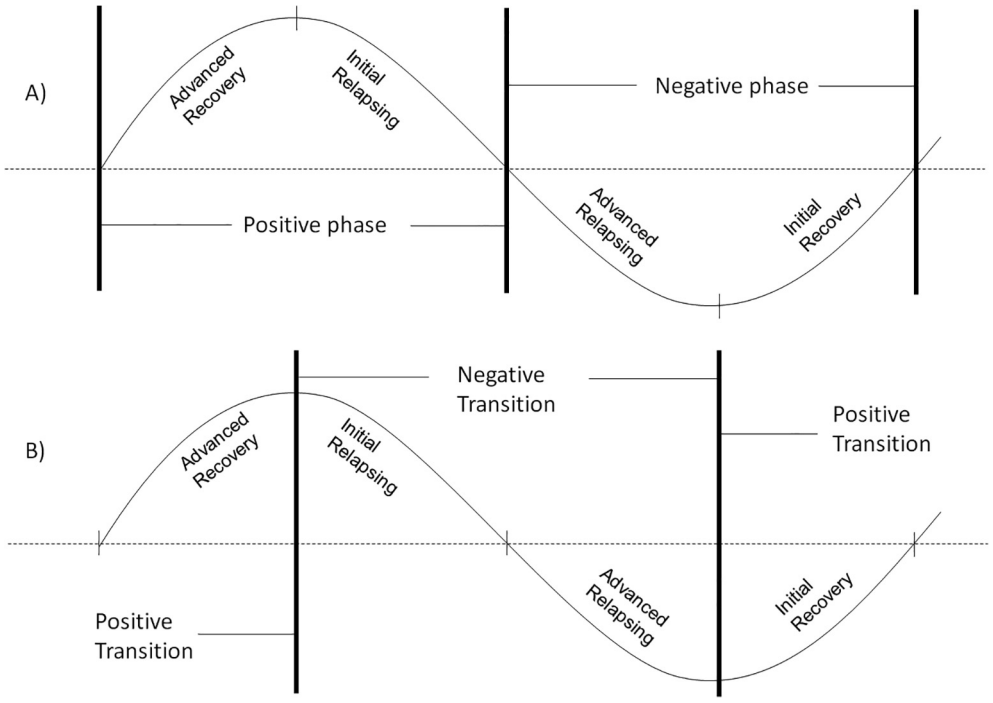

Fig. 4. Trend-Cycle phases as defined by: A) Cyclic phases: Positive phase (Advanced Recovery and Initial Relapsing), and Negative phase (Advanced Relapsing and Initial Recovery), and B) Transitions: Positive transition (Initial Recovery and Advanced Recovery), and Negative transition (Initial Relapsing and Advanced Relapsing).

values at the end of the time series (Fig. 6C, D). This was evidenced in the high proportion of the total area that recorded a positive trend-cycle (with highest proportions in San Jorge Gulf shrublands, Austral and Eastern Monte biozones, Fig. 5) and predominantly in a Departure stage (98%) from the negative phase (Table 2). A complementary interpretation of this scenario is that almost half of Patagonian area is situated in an Early stage (98%) of a negative transition, which may reference a potential future downward movement. On the other hand, Initial Recovery was mostly recorded in Valdes Peninsula and Western Hills and Plateaus Steppes biozones, which registered the highest proportions of area in Early stage (> 70%) of a positive transition. This scenario is explained by the strong disturbance originated by the interaction between drought and ash fallout from the Puyehue-Cordón Caulle Volcanic Complex eruption in 2011 in North Patagonia, which significantly affected vegetation productivity dynamics and a delayed recovery (Easdale and Bruzzone, 2018).

5. Discussion

We assessed NDVI trend-cycles as proxies for land dynamics in Patagonia, Argentina. NDVI trend-cycle explained a significant portion of temporal variability, reaching almost 20% of time series information. This proportion of explained information was at least 6-fold higher than previous studies that considered only NDVI trends using wavelets (Easdale et al. 2018). Monotonic patterns and particularly decreasing trend-cycles were marginally recorded, indicating that a negative regime shift was not a dominant pattern in the last 18 years of NDVI records and contradicting current wisdom on land assessment in dryland Patagonia (e.g., Gaitán et al., 2015). Moreover, most patterns identified referred to different cycle phases as measured by non-monotonic functions (Table 2). These results suggest that trend-cycle is a sensitive method in capturing medium term oscillations around a long-term movement of land dynamics, as measured by NDVI time series. For instance, most trend-cycles were classified as Initial or Advanced Recovery and Initial Relapsing, which are different positions within a positive phase or pulse of a recent increase in primary productivity of rangelands in Patagonia. These situations can be synthesized in two main interpretations of the same phenomenon, mainly driven by climate as recorded in other regions worldwide (Nemani et al., 2003). Dryland Patagonia is experiencing a changing phase from minimum NDVI values that occurred in the midsection of the time series (e.g. spatially varying between years 2009 and 2016, Fig. 6), followed by increasing NDVI values towards the end of the 18-years series. Environmental drivers such as a long-lasting drought that affected Patagonia between 2008 and 2013 may explain differences in the magnitude and duration of the fall in the time series (Fig. 6A, D; Easdale and Rosso 2010). As well, the interaction between drought and volcanic ash deposits from the Puyehue-Cordón Caulle Volcanic Complex eruption in 2011 caused a major disturbance in a large area of North Patagonia (Figs. 5 and 6B; Collini et al., 2013; Easdale and Bruzzone 2018). On the other hand, a positive pulse was evident from the year 2014 onward, which may be explained by higher regional rainfalls. These results of trend-cycle analysis can inform how ecological systems change during short and long term disturbances or environmental changes (Pettorelli et al., 2005; Nimmo et al., 2015). The relationship between explanatory factors and trend-cycles needs more study. However, these results are encouraging as a step towards the development of a tool for regional land monitoring.

Global tools to monitor land degradation in drylands is one of the main challenges of international agreements (Grainger, 2015). One of the current methods mostly used to evaluate the interplay between Sustainable Land Management (SLM) and indicators obtained from satellite-based earth observation, is based on indicators derived from annual integrals of NDVI (such as Trends.Earth). A recent assessment concluded that only technologies with more than 10 years since implementation showed statistically significant improvements (Gonzalez-Roglich et al., 2019). We acknowledge the long time needed to record evidence of positive changes in land productivity indicators as a result of SLM practices. However, two main methodological limitations are that trends explain a marginal portion of the variability in NDVI series, and that medium-term changes cannot be identified with monotonic, linear trends derived from annual integrals of NDVI (Easdale et al., 2018). Trend-cycle can be an alternative method to overcome these limitations. In particular, the main strength relies in its sensitivity to capture medium-term fluctuations around the long-term movement of NDVI temporal dynamics. Then, it can provide scenario information using all available time series data with high opportunities to identify medium-term changes (i.e. four or five years' phases) in the light of

Table 2
Proportion of area (%) of different trend-cycle classes for each Patagonian biozone. Trend-cycle phases as defined by (Fig. 3): A) Cyclic phases: Positive phase (Advanced Recovery –Positive Entry Stage– and Initial Relapsing –Positive Departure Stage–), and Negative phase (Advanced Relapsing –Negative Entry Stage– and Initial Recovery –Negative Departure Stage–), and B) Transitions: Positive transition (Initial Recovery –Positive Early Stage– and Advanced Recovery –Positive Consolidated Stage–), and Negative transition (Initial Relapsing –Negative Early Stage– and Advanced Relapsing –Negative Consolidated Stage).

Trend-Cycle	Andes	Central Plateau Steppes	Western Hills & Plateaus Steppes	Austral Monte Shrublands	Eastern Monte Shrublands	Subandean Grasslands	San Jorge Gulf Shrublands	Valdes Peninsula	Irrigated Valleys	Humid Magellan Steppe	Dry Magellan Steppe	Mulguraea Shrublands	Tierra del Fuego Ecotone	Patagonia ($x10^3$ ha)
Decreasing	0.4	0.0	0.1	0.0	0.1	0.3	0.0	0.1	0.1	0.0	0.0	0.0	0.0	0.1
Initial Recovery	24.7	27.8	40.0	30.9	23.3	26.8	27.9	57.4	25.7	23.9	28.0	20.2	28.0	29.7
Advanced Relapsing	1.0	0.6	1.0	0.6	0.6	0.8	0.3	0.8	0.9	0.2	0.1	0.1	0.1	0.6
Advanced Recovery	17.2	23.5	14.8	15.8	11.6	16.3	31.5	9.3	16.4	15.5	23.7	23.1	6.3	19.1
Initial Relapsing	26.3	32.5	31.6	51.4	63.0	24.7	36.2	28.8	52.0	34.4	26.9	23.5	38.8	36.1
Increasing	1.2	0.8	0.6	0.1	0.1	0.8	0.5	0.1	0.5	0.4	0.1	0.3	0.4	0.6
No Trend-Cycle	29.2	14.9	12.0	1.2	1.3	30.3	3.5	3.5	4.4	25.6	21.1	32.8	26.4	13.8
Total Area ($x10^3$ ha)	6,091	26,900	12,401	15,250	2,861	5,007	2,630	388	685	1,028	1,175	2,842	487	77,746
Trend-Cycle Phase														
Negative Phase	***25.7***	***28.4***	***40.9***	***31.5***	***23.9***	***27.7***	***28.3***	***58.2***	***26.6***	***24.1***	***28.1***	***20.3***	***28.1***	***30.3***
Entry stage (-)	3.8	2.0	2.4	1.9	2.5	3.0	1.1	1.4	3.3	0.7	0.4	0.3	0.4	2.1
Departure stage (-)	96.2	98.0	97.6	98.1	97.5	97.0	98.9	98.6	96.7	99.3	99.6	99.7	99.6	97.9
Positive Phase	***43.5***	***56.0***	***46.4***	***67.2***	***74.6***	***41.0***	***67.7***	***38.2***	***68.4***	***49.9***	***50.7***	***46.6***	***45.0***	***55.2***
Entry stage (+)	39.6	41.9	31.9	23.5	15.6	39.7	46.5	24.5	24.0	31.0	46.9	49.5	13.9	34.6
Departure stage (+)	60.4	58.1	68.1	76.5	84.4	60.3	53.5	75.5	76.0	69.0	53.1	50.5	86.1	65.4
No Trend-Cycle	***29.2***	***14.9***	***12.0***	***1.2***	***1.3***	***30.3***	***3.5***	***3.5***	***4.4***	***25.6***	***21.1***	***32.8***	***26.4***	***13.8***
Monotonic change	***1.6***	***0.8***	***0.6***	***0.1***	***0.1***	***1.1***	***0.5***	***0.2***	***0.6***	***0.4***	***0.1***	***0.3***	***0.4***	***0.6***
Trend-Cycle Transition														
Negative Transition	***41.9***	***51.3***	***54.8***	***46.7***	***34.9***	***43.1***	***59.5***	***66.7***	***42.2***	***39.4***	***51.7***	***43.3***	***34.3***	***48.8***
Early stage (-)	96.5	98.3	97.0	98.8	99.0	96.8	99.1	97.3	98.4	99.5	99.5	99.7	99.7	98.2
Consolidated stage (-)	3.5	1.7	3.0	1.2	1.0	3.2	0.9	2.7	1.6	0.5	0.5	0.3	0.3	1.8
Positive Transition	***27.2***	***33.1***	***32.6***	***52.0***	***63.6***	***25.5***	***36.5***	***29.6***	***52.9***	***34.6***	***27.0***	***23.6***	***38.9***	***36.8***
Early stage (+)	59.0	54.2	73.0	66.2	66.7	62.2	47.00	86.0	61.0	60.8	54.1	46.7	81.7	60.8
Consolidated stage (+)	41.0	45.8	27.0	33.8	33.3	37.8	53.0	14.0	39.0	39.2	45.9	53.3	18.3	39.2
No Trend-Cycle	***29.2***	***14.9***	***12.0***	***1.2***	***1.3***	***30.3***	***3.5***	***3.5***	***4.4***	***25.6***	***21.1***	***32.8***	***26.4***	***13.8***
Monotonic change	***1.6***	***0.8***	***0.6***	***0.1***	***0.1***	***1.1***	***0.5***	***0.2***	***0.6***	***0.4***	***0.1***	***0.3***	***0.4***	***0.6***

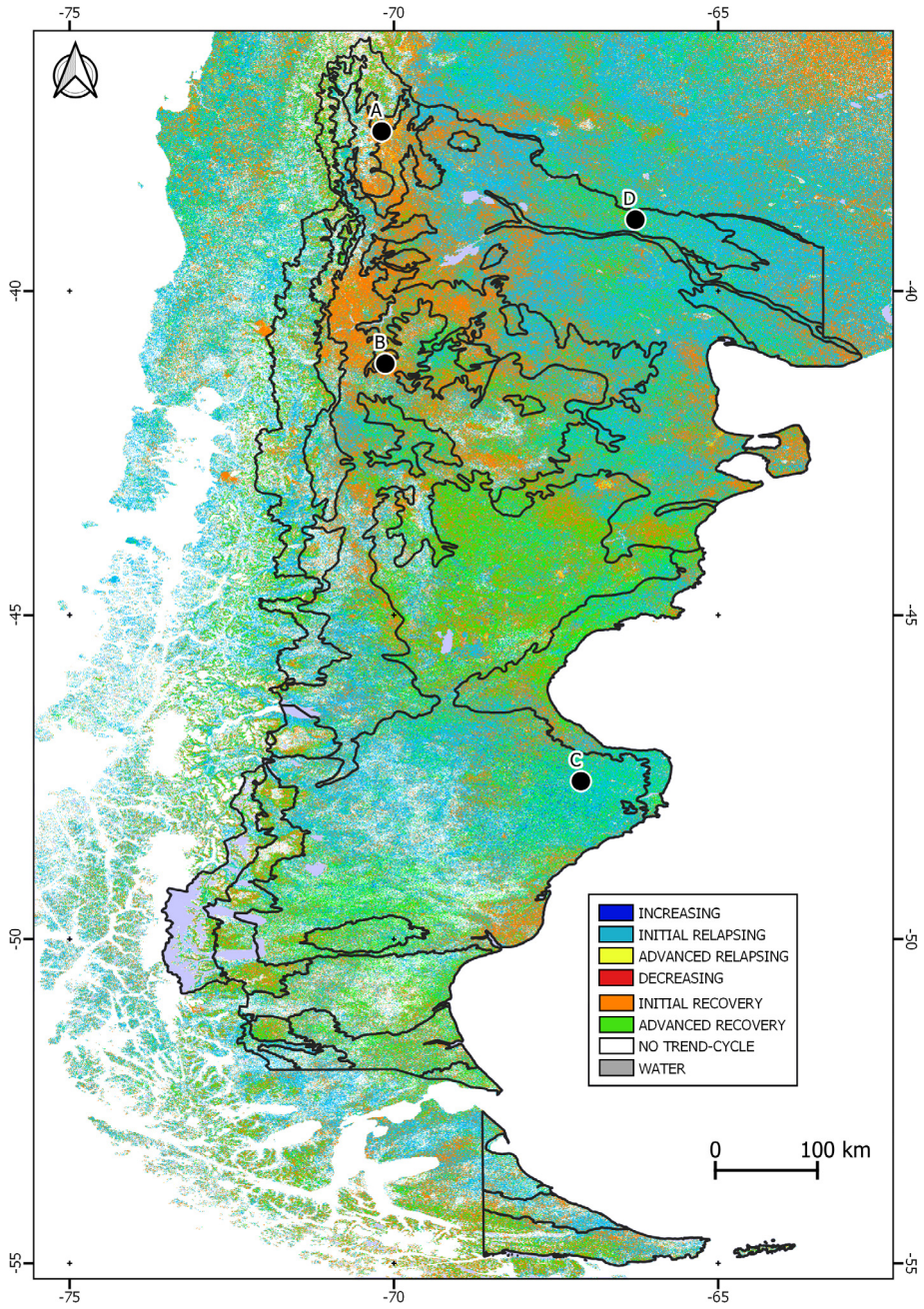

Fig. 5. NDVI Trend-cycles classification for Patagonia, Argentina: i) Increasing (blue), ii) Initial Relapsing (light blue), iii) Advanced Relapsing (yellow), iv) Advanced Recovery (green), v) Initial Recovery (orange), vi) Decreasing (red), vii) No Trend-Cycle (white). Black lines identify the boundaries of biozones (Fig. 1). Data source: MODIS images for the time series between 2000-mid-2018.

long-term monotonic and non-monotonic trends (> 10 years). More research is needed to assess the capacity as a monitoring system to capture the interaction between the impact of SLM practices on primary productivity and environmental changes at finer spatial and temporal scales (Gonzalez-Roglich et al., 2019).

Trend-cycle analysis may also function as an early warning tool to inform decision-makers at a coarser scale and support adaptive land management as strategies for SLM at a regional scale. For example, areas with Initial Relapsing patterns refer to a near-maximum NDVI values and a shift in the direction of the medium-term movement, from increasing to decreasing. Whereas the future behaviour should be closely monitored, a scenario of Advanced Relapsing can follow this shift (Fig. 4), which may confirm a negative transition phase for the upcoming years. Regional pastoral livestock farmers, which strongly rely on rangeland productivity, should be aware of this scenario. In particular, public policy and farm management should be modified from a position dominated by "managing the abundance" towards a position that prioritizes "anticipating the impact" of a drier or negative phase, depicted by a forthcoming reduction of rangeland productivity and forage (e.g. a potential future scenario for the Monte shrublands, Table 2). In other words, decisions should be oriented at preventing or minimizing a future livestock productivity loss or even a decapitalization process (i.e. if livestock die), and the subsequent socio-economic impacts (Oba, 2001). On the other hand, areas with Initial Recovery patterns refer to a recent near-minimum NDVI values (which reflect a perturbation impact such as drought, e.g. Easdale and Rosso, 2010), with an initial shift towards a positive pulse or phase in rangeland productivity dynamics (Fig. 6B). In these cases, farm management

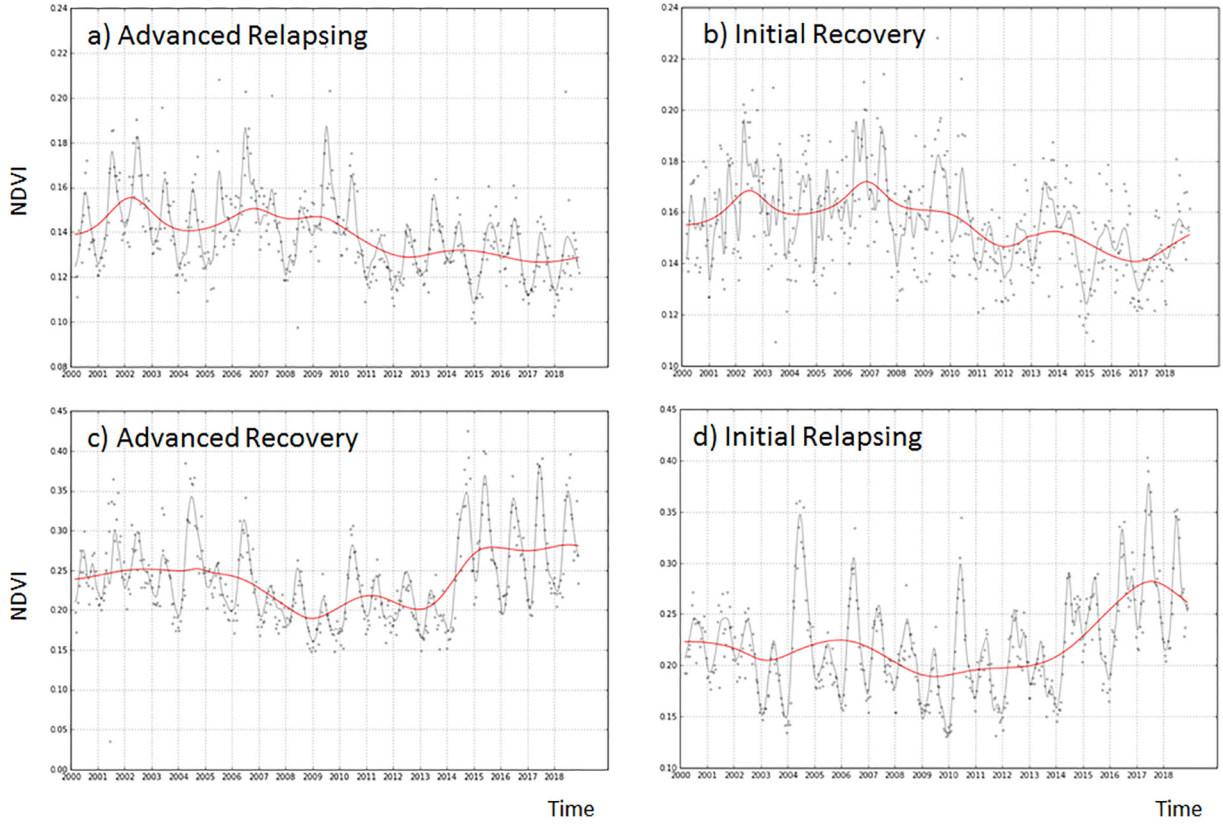

Fig. 6. NDVI Trend-cycle classified as: (A) Advanced Relapsing for a pixel series situated in −70.19, −37.53; (B) Initial Recovery for a pixel series situated in −70.13, −41.12; (C) Advanced Recovery for a pixel series situated in −67.11, −47.56; (D) Initial Relapsing for a pixel series situated in −66.27, −38.89. Grey dots indicate original data, grey line the annual function and red line identifies the trend-cycle function. Spatial location of pixels is provided in Fig. 5.

should prioritize rangeland recovery (Ares, 2007) and public policy be oriented at helping rural households in fostering their social-ecological resilience instead of promoting a rapid restocking (Domptail et al., 2013). Trend-cycle approach can also complement SLM in providing a full description of rangeland dynamics, exceeding the annual cycle as the main productive period. For instant, management adaptations based on varying stocking rates, strategic supplementary feeding (i.e. for some animal categories or key moments such as pre-lambing), water reservoirs and rotational rangeland management can be defined considering both annual plans and a trend-cycle approach to include medium-term scenarios.

This regional monitoring tool can be used to complement other sources of information such as meteorological and field data. For instance, vegetation and soil data gathered every five years with a field monitoring tool (Oliva et al., 2019), can be better interpreted in the light of trend-cycle class of each monitor, at the moment of sampling. However, we emphasize that further research is needed to separate NDVI time series into other different components, which were not tackled with trend-cycle, such as high and other low frequency domains as measures of periodic components, stochastic components and white noise (Jakubauskas et al., 2001; Hird and McDermid, 2009; Verbesselt et al., 2010).

6. Conclusions

Trend-cycle is a sensitive method to capture medium-term fluctuations around the long-term movement of temporal dynamics such as NDVI time series. Its performance was tested in a large and heterogeneous region such as Patagonia, Argentina. From our findings, trend-cycle may contribute to overcome two main limitations of current dominant NDVI trend analysis. First, to increase the marginal explanatory capacity provided by trends in relation to the total temporal information of NDVI time series. Second, to include medium-term changes and oscillations associated to ecosystem cyclic phases or perturbations that influence the long-term behaviour, but which cannot be identified with linear trends derived from annual integrals of NDVI. Given the width of the temporal window of remote sensing data, the integration of trend and inter-annual cycles seems to be more adequate to better capturing medium to long-term land dynamics. Whereas trend-cycle needs more research, it has potential as a tool to monitor land dynamics and progress towards land degradation neutrality.

Acknowledgements

This research was funded by Instituto Nacional de Tecnología Agropecuaria (INTA) and Ministerio de Ciencia, Tecnología e Innovación Productiva Argentina (PICT 2015-929). We warmly thank two anonymous reviewers for their helpful comments and suggestions, which improved the readability of this article.

References

Aguiar, M.R., Paruelo, J.M., Sala, O.E., Lauenroth, W.K., 1996. Ecosystem responses to changes in plant functional type composition: an example from the Patagonian steppe. J. Veg. Sci. 7 (3), 381–390.

Anyamba, A., Tucker, C.J., 2005. Analysis of Sahelian vegetation dynamics using NOAA-AVHRR NDVI data from 1981–2003. J. Arid Environ. 63 (3), 596–614. https://doi.org/10.1016/j.jaridenv.2005.03.007.

Ares, J.O., 2007. Systems valuing of natural capital and investment in extensive pastoral systems: lessons from the Patagonian case. Ecol. Econ. 62 (1), 162–173.

Ashton, W.D., 1972. The logit transformation: with special reference to its uses in Bioassay. In: Griffin's Statistical Monographs & Courses, vol. 32. Charles Griffin, London UK, pp. 88.

Bai, Z.G., Dent, D.L., Olsson, L., Schaepman, M.E., 2008. Proxy global assessment of land degradation. Soil Use Manag. 24 (3), 223–234. https://doi.org/10.1111/j.1475-2743.2008.00169.x.

Beck, H.E., McVicar, T.R., van Dijk, A.I., Schellekens, J., de Jeu, R.A., Bruijnzeel, L.A.,

2011. Global evaluation of four AVHRR–NDVI data sets: intercomparison and assessment against Landsat imagery. Remote Sens. Environ. 115 (10), 2547–2563. https://doi.org/10.1016/j.rse.2011.05.012.
Bran, D., Oliva, G., Rial, P., Escobar, J., López, C., Umaña, F., Ayesa, J., Elissalde, N. 2005. Regiones Ecológicas Homogéneas de la Patagonia Argentina. Comunicación Técnica Relevamiento Integrado N°132, Área Recursos Naturales. INTA, 12 pp.
Bruzzone O., Easdale M.H. 2018. Gpu_pursuit, version 0.2, Zenodo. DOI: 10.5281/zenodo.1283338.
Chen, S.S., Donoho, D.L., Saunders, M.A., 2001. Atomic decomposition by basis pursuit. SIAM Rev. 43 (1), 129–159.
Collini, E., Osores, M.S., Folch, A., Viramonte, J.G., Villarosa, G., Salmuni, G., 2013. Volcanic ash forecast during the June 2011 Cordón Caulle eruption. Nat. Hazards 66 (2), 389–412. https://doi.org/10.1007/s11069-012-0492-y.
de Jong, R., de Bruin, S., de Wit, A., Schaepman, M.E., Dent, D.L., 2011. Analysis of monotonic greening and browning trends from global NDVI time-series. Remote Sens. Environ. 115 (2), 692–702. https://doi.org/10.1016/j.rse.2010.10.011.
Demanet, L., Ying, L., 2007. Wave atoms and sparsity of oscillatory patterns. Appl. Comput. Harmon. Anal. 23 (3), 368–387. https://doi.org/10.1016/j.acha.2007.03.003.
del Valle, H.F., Elissalde, N.O., Gagliardini, D.A., Milovich, J., 1998. Status of desertification in the Patagonian region: assessment and mapping from satellite imagery. Arid Soil Res. Rehabil. 12, 1–27.
Easdale, M.H., Aguiar, M.R., Román, M., Villagra, S.E., 2009. Comparación socio-económica de dos regiones biofísicas: los sistemas ganaderos de Río Negro, Argentina. Cuadernos de Desarrollo Rural 62, 173–198.
Domptail, S., Easdale, M.H., Yuerlita, 2013. Managing socio-ecological systems to achieve sustainability: a study of resilience and robustness. Environ. Policy Governance 23 (1), 30–45.
Easdale, M.H., Rosso, H., 2010. Dealing with drought: social implications of different smallholder survival strategies in semi-arid rangelands of Northern Patagonia, Argentina. Rangeland J. 32 (2), 247–255.
Easdale, M.H., Sacchero, D., Vigna, M., Willems, P., 2014. Assessing the magnitude of impact of volcanic ash deposits on Merino wool production and fibre traits in the context of a drought in North-west Patagonia, Argentina. Rangeland J. 36 (2), 143–149.
Easdale, M.H., Bruzzone, O., Mapfumo, P., Tittonell, P., 2018. Phases or regimes? Revisiting NDVI trends as proxies for land degradation. Land Degrad. Dev. 29 (3), 433–445.
Easdale, M.H., Bruzzone, O., 2018. Spatial distribution of volcanic ash deposits of 2011 Puyehue-Cordón Caulle eruption in Patagonia as measured by a perturbation in NDVI temporal dynamics. J. Volcanol. Geoth. Res. 353, 11–17.
Eckert, S., Hüsler, F., Liniger, H., Hodel, E., 2015. Trend analysis of MODIS NDVI time series for detecting land degradation and regeneration in Mongolia. J. Arid Environ. 113, 16–28. https://doi.org/10.1016/j.jaridenv.2014.09.001.
Eklundh, L., Olsson, L., 2003. Vegetation index trends for the African Sahel 1982–1999. Geophys. Res. Lett. 30 (8).
Fensholt, R., Langanke, T., Rasmussen, K., Reenberg, A., Prince, S.D., Tucker, C., Scholes, R.J., Le, Q.B., Bondeau, A., Eastman, R., Epstein, H., 2012. Greenness in semi-arid areas across the globe 1981–2007—An earth observing satellite based analysis of trends and drivers. Remote Sens. Environ. 121, 144–158. https://doi.org/10.1016/j.rse.2012.01.017.
Fletcher, R., 1987. Practical Methods of Optimization. John Wiley & Sons, New York, pp. 436.
Gabor, D., 1946. Theory of communication. J. Inst. Electr. Eng. 93, 429–441.
Gaitán, J.J., Bran, D., Oliva, G., Ciari, G., Nakamatsu, V., Salomone, J., Ferrante, D., Buono, G., Massara, V., Humano, G., Celdrán, D., Opazo, W., Maestre, F.T., 2013. Evaluating the performance of multiple remote sensing indices to predict the spatial variability of ecosystem structure and functioning in Patagonian steppes. Ecol. Ind. 34, 181–191. https://doi.org/10.1016/j.ecolind.2013.05.007.
Gaitán, J.J., Bran, D.D., Azcona, C., 2015. Tendencia del NDVI en el período 2000–2014 como indicador de la degradación de tierras en Argentina: ventajas y limitaciones. AGRISCIENTIA 32 (2), 83–93.
Gill, P.R., Wang, A., Molnar, A., 2011. The in-crowd algorithm for fast basis pursuit denoising. IEEE Trans. Signal Process. 59 (10), 4595–5460.
Gonzalez-Roglich, M., Zvoleff, A., Noon, M., Liniger, H., Fleiner, R., Harari, N., Garcia, C., 2019. Synergizing global tools to monitor progress towards land degradation neutrality: trends. Earth and the world overview of conservation approaches and technologies sustainable land management database. Environ. Sci. Policy 93, 34–42. https://doi.org/10.1016/j.envsci.2018.12.019.
Grainger, A., 2015. Is land degradation neutrality feasible in dry areas? J. Arid Environ. 112, 14–24.
Hák, T., Janoušková, S., Moldan, B., 2016. Sustainable development goals: a need for relevant indicators. Ecol. Ind. 60, 565–573.
Hird, J.N., McDermid, G.J., 2009. Noise reduction of NDVI time series: an empirical comparison of selected techniques. Remote Sens. Environ. 113 (1), 248–258. https://doi.org/10.1016/j.rse.2008.09.003.
Hunter, J.D., 2007. Matplotlib: A 2d graphics environment. Comput. Sci. Eng. 9 (3), 90–95.
Hurvich, C.M., Tsai, C.L., 1989. Regression and time series model selection in small samples. Biometrika 76 (2), 297–307.
Jakubauskas, M.E., Legates, D.R., Kastens, J.H., 2001. Harmonic analysis of time-series AVHRR NDVI data. Photogramm. Eng. Remote Sens. 67 (4), 461–470.
Jamali, S., Seaquist, J., Eklundh, L., Ardö, J., 2014. Automated mapping of vegetation trends with polynomials using NDVI imagery over the Sahel. Remote Sens. Environ. 141, 79–89. https://doi.org/10.1016/j.se.2013.10.019.
Jobbágy, E.G., Sala, O.E., 2000. Controls of grass and shrub aboveground production in the Patagonian steppe. Ecol. Appl. 10 (2), 541–549.
León, R., Bran, D., Collantes, M., Paruelo, J.M., Soriano, A., 1998. Grandes unidades de vegetación de la Patagonia. Ecología Austral 8 (2), 125–144.
Liu, S., Wang, T., Kang, W., David, M., 2015. Several challenges in monitoring and assessing desertification. Environ. Earth Sci. 73 (11), 7561–7570.
Luo, H., Tang, Y., Zhu, X., Di, B., Xu, Y., 2016. Greening trend in grassland of the Lhasa River Region on the Qinghai-Tibetan Plateau from 1982 to 2013. Rangeland J. 38 (6), 591–603.
Mallat, S., 1999. A Wavelet Tour of Signal Processing, 2nd Edition. Academic Press, Elsevier, UK 832pp.
Metternicht, G., Zinck, J.A., Blanco, P.D., Del Valle, H.F., 2010. Remote sensing of land degradation: experiences from Latin America and the Caribbean. J. Environ. Qual. 39, 42–61. https://doi.org/10.2134/jeq2009.0127.
Mazzonia, E., Vazquez, M., 2009. Desertification in Patagonia. Devel. Earth Surface Processes 13, 351–377.
Millennium Ecosystem Assessment, 2005. Ecosystems and human well-being: our human planet: summary for decision-makers, vol. 5 Island Press, Washington.
Miao, C.Y., Yang, L., Chen, X.H., Gao, Y., 2012. The vegetation cover dynamics (1982–2006) in different erosion regions of the Yellow River Basin, China. Land Degrad. Dev. 23, 62–71. https://doi.org/10.1002/ldr.1050.
Nelson, C.R., 2010. Trend/Cycle decomposition. In: Durlauf, S.N., Blume, L.E. (Eds.), Macroeconometrics and Time Series Analysis. The New Palgrave Economics Collection, Palgrave Macmillan, London, pp. 343–346.
Nemani, R.R., Keeling, Ch.D., Hashimoto, H., Jolly, W.M., Piper, S.C., Tucker, C.J., Myneni, R.B., Running, S.W., 2003. Climate-driven increases in global terrestrial net primary production from 1982 to 1999. Science 300 (5625), 1560–1563. https://doi.org/10.1126/science.1082750.
Nimmo, D.G., Mac Nally, R., Cunningham, S.C., Haslem, A., Bennett, A.F., 2015. Vive la résistance: reviving resistance for 21st century conservation. Trends Ecol. Evol. 30 (9), 516–523.
Oba, Gufu, 2001. The effect of multiple droughts on cattle in Obbu, Northern Kenya. J. Arid Environ. 49 (2), 375–386.
Oliva, G., Bran, D., Gaitán, J., Ferrante, D., Massara, V., García Martínez, G., Adema, E., Enrique, M., Domínguez, E., Paredes, P., 2019. Monitoring drylands: The MARAS system. J. Arid Environ. 161, 55–63. https://doi.org/10.1016/j.jaridenv.2018.10.004.
Omuto, C.T., Balint, Z., Alim, M.S., 2014. A framework for national assessment of land degradation in the drylands: a case study of Somalia. Land Degrad. Dev. 25, 105–119. https://doi.org/10.1002/ldr.1151.
Oñatibia, G.R., Aguiar, M.R., 2016. Continuous moderate grazing management promotes biomass production in Patagonian arid rangelands. J. Arid Environ. 125, 73–79.
Paruelo, J.M., Aguiar, M.R., Golluscio, R.A., León, R., 1992. La Patagonia extrandina: análisis de la estructura y el funcionamiento de la vegetación a distintas escalas. Ecología Austral 2 (2), 123–136.
Peters, D.P., Bestelmeyer, B.T., Herrick, J.E., Fredrickson, E.L., Monger, H.C., Havstad, K.M., 2006. Disentangling complex landscapes: new insights into arid and semiarid system dynamics. Bioscience 56 (6), 491–501.
Pettorelli, N., Vik, J.O., Mysterud, A., Gaillard, J.M., Tucker, C.J., Stenseth, N.C., 2005. Using the satellite-derived NDVI to assess ecological responses to environmental change. Trends Ecol. Evol. 20 (9), 503–510. https://doi.org/10.1016/j.tree.2005.05.011.
Rouse, J.W., Haas, R.H., Schell, J.A., Deering, D.W., 1973. Monitoring vegetation systems in the great plains with ERTS. In: Third ERTS Symposium, NASA SP-351 I, pp. 309–317.
Saha, M.V., Scanlon, T.M., D'Odorico, P., 2015. Examining the linkage between shrub encroachment and recent greening in water-limited southern Africa. Ecosphere 6 (9), 156. https://doi.org/10.1890/ES15-00098.1.
Scheffer, M., Carpenter, S.R., 2003. Catastrophic regime shifts in ecosystems: linking theory to observation. Trends Ecol. Evol. 18 (12), 648–656.
Tucker, C.J., 1979. Red and photographic infrared linear combinations for monitoring vegetation. Remote Sensing Environ. 8, 681–698.
Van Eaton, A.R., Amigo, Á., Bertin, D., Mastin, L.G., Giacosa, R.E., González, J., Valderrama, O., Fontijn, K., Behnke, S.A., 2016. Volcanic lightning and plume behavior reveal evolving hazards during the April 2015 eruption of Calbuco volcano, Chile. Geophys. Res. Lett. 43 (7), 3563–3571. https://doi.org/10.1002/2016GL068076.
Verbesselt, J., Hyndman, R., Newnham, G., Culvenor, D., 2010. Detecting trend and seasonal changes in satellite image time series. Remote Sens. Environ. 114 (1), 106–115. https://doi.org/10.1016/j.rse.2009.08.014.
Verón, S.R., Paruelo, J.M., 2010. Desertification alters the response of vegetation to changes in precipitation. J. Appl. Ecol. 47 (6), 1233–1241.
Villagra, S.E, Easdale, M.H., Bolla, D., 2008. Efectos de la sequía sobre la situación de la ganadería extensiva de la provincia de Río Negro. INTA Bariloche, Comunicación Técnica SPES 223, 18pp.
Vogt, J.V., Safriel, U., Von Maltitz, G., Sokona, Y., Zougmore, R., Bastin, G., Hill, J., 2011. Monitoring and assessment of land degradation and desertification: Towards new conceptual and integrated approaches. Land Degrad. Dev. 22, 150–165. https://doi.org/10.1002/ldr.1075.
Vlek, P., Bao Le, Q., Tamene, L., 2008. Land decline in Land Rich Africa – A creeping disaster in the making. CGIAR Science Council Secretariat, Rome, Italy.
Watt, S.F., Pyle, D.M., Mather, T.A., Martin, R.S., Matthews, N.E., 2009. Fallout and distribution of volcanic ash over Argentina following the May 2008 explosive eruption of Chaitén, Chile. J. Geophys. Res. Solid Earth 114 (B4).
Wessels, K.J., Prince, S.D., Malherbe, J., Small, J., Frost, P.E., VanZyl, D., 2007. Can human-induced land degradation be distinguished from the effects of rainfall variability? A case study in South Africa. J. Arid Environ. 68 (2), 271–297. https://doi.

org/10.1016/j.jaridenv.2006.05.015.
Wessels, K.J., van den Bergh, F., Scholes, R.J., 2012. Limits to detecting of land degradation by trend analysis of vegetation index data. Remote Sens. Environ. 125, 10–22.
Yin, H., Udelhoven, T., Fensholt, R., Pflugmacher, D., Hostert, P., 2012. How Normalized Difference Vegetation Index (NDVI) trends from Advanced Very High Resolution Radiometer (AVHRR) and Système Probatoire d'Observation de la Terre VEGETATION (SPOT VGT) time series differ in agricultural areas: an inner mongolian case study. Remote Sensing 4, 3364–3389. https://doi.org/10.3390/rs4113364.
Zoungrana, B.J., Conrad, C., Thiel, M., Amekudzi, L.K., Da, E.D., 2018. MODIS NDVI trends and fractional land cover change for improved assessments of vegetation degradation in Burkina Faso, West Africa. J. Arid Environ. 153, 66–75.